

Fundamental Study on Near-Field Effects on Earthquake Response of Arch Dams

Tatsuo Ohmachi ¹⁾ Abdolrahim Jalali ²⁾

1) Professor, Department of Built Environment, Interdisciplinary Graduate School of Science and Engineering, Tokyo Institute of Technology, Yokohama, Japan.

2) Ph.D. student, Department of Built Environment, Interdisciplinary Graduate School of Science and Engineering, Tokyo Institute of Technology, Yokohama, Japan.

ABSTRACT

Effects of directivity of near-field and vertical ground motion on linear response of an arch dam are studied. In investigating directivity, the variation of stresses at all elements on upstream and downstream face of the dam due to different angle of incident are studied. The dam stresses are found to show remarkable increase or decrease at special angle of incident with respect to the case of imposing the recorded ground motion in upstream, vertical, and cross-stream (the case which corresponds to angle of incident = 0 in this study). In the case of vertical ground motion, the contribution of vertical ground motion on arch, cantilever, and principal stresses of total response is considered. Results show little contribution (about 30%) from vertical ground motion, compared with contribution from upstream component for this special case.

INTRODUCTION

Numerous failures to civil engineering structures were observed in the near-field of the 1994 Northridge, California earthquake and the 1995 Hyogoken-Nanbu, Japan earthquake. According to post earthquake studies [1~5], some of the overwhelming failures are attributed to near-field effects of the earthquake ground motion, and many experts point out that the near-field effects should be adequately taken into account in seismic structural design as soon as possible.

In comparison with the far-field motions, some of unique features of the near-field ground motions have been identified by many researchers are:

1. One or multiple distinctive large pulses occur at the beginning of the S-wave motion with rather short duration.
2. The large pulse of the motion is polarized in the direction normal to the fault strike, which is often referred to as directivity.
3. The pulse of the motion shows large amplitude in both horizontal and vertical directions, which sometimes

amounts to 1 g in acceleration and 1 m/s in velocity.

In general, nonlinear structural response analysis will be required to identify damaging characteristics of near-field motions. In particular, regarding earthquake response of arch dams, several important factors have been pointed out in previous studies [6~9], such as opening of contraction and lift joints, non-uniform input motion and canyon topography. These factors, however, do not seem to be adequate to represent the effects of above features of the near-field motion. On this basis, this study deals with response of an arch dam to a near-field ground motion actually observed at a dam site, although it is limited within linear behavior. The main objective of this study is to evaluate ranges of variation in stresses due to the directivity and vertical component of the motion, which will be one of the key factors in the seismic design of the structure.

INPUT GROUND MOTION

The ground motions recorded at Pacoima Dam Station during the Northridge earthquake, January 17, 1994 is selected as the ground acceleration for the analysis in this study. The recorded ground motions consist of the three components in the upstream (S 85°W), vertical, and cross-stream (S 5°E) directions, respectively. Time histories and response spectra of the ground motions are shown in Figs. 1 and 2. A trace of the two horizontal components is shown in Fig. 3, from which the directivity of the motion is evident.

To consider the effect of directivity of near-field ground motion, on response of an arch dam, we have considered several positions for dam with respect to

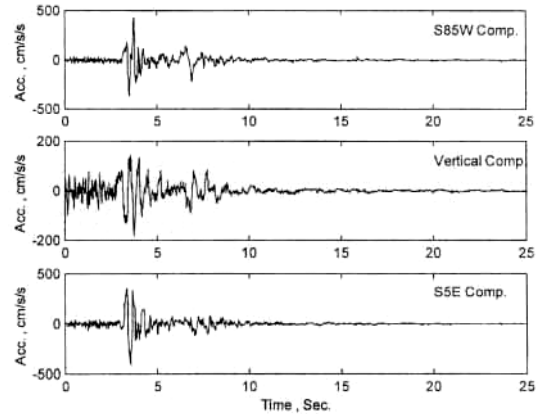


Fig. 1 Ground motions at Pacoima Dam St., Northridge Earthquake, 17 Jan. 1994

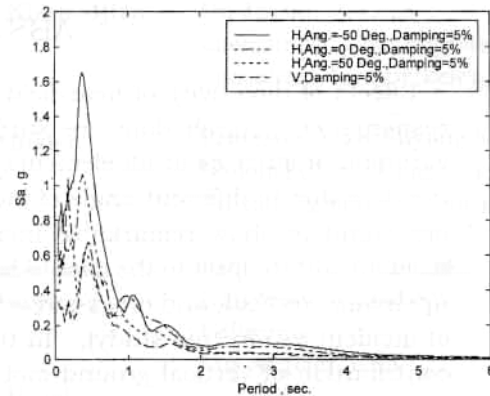


Fig. 2 Response spectra for horizontal (H) and vertical (V) components of input ground motion

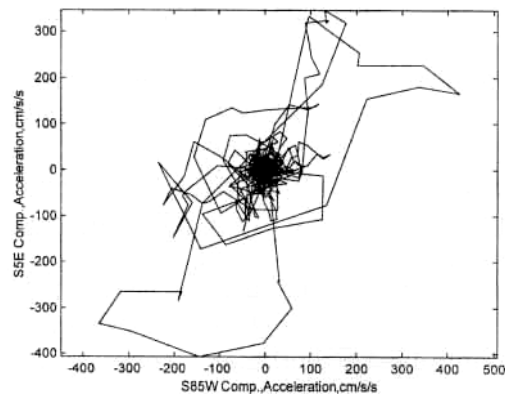


Fig. 3 Trace of horizontal components of input ground motion

horizontal components of ground motion. To handle the problem easily, instead of rotating the dam, we have considered transformation of horizontal components of ground motion by rotating the incident angle of the original ground motion from $\beta = -90^\circ$ to $\beta = +150^\circ$, as shown in Fig. 4. When $\beta = 0^\circ$, the upstream, vertical, and cross-stream ground motions, are denoted by $a_g^x(t)$, $a_g^y(t)$, and $a_g^z(t)$. The relation between two sets of accelerations in the two sets of coordinate systems ZX and $Z'X'$, shown in Fig. 4, is given as following:

$$\begin{cases} a_g^{x'}(t) \\ a_g^{z'}(t) \end{cases} = \begin{bmatrix} \cos \beta & -\sin \beta \\ \sin \beta & \cos \beta \end{bmatrix} \begin{cases} a_g^x(t) \\ a_g^z(t) \end{cases} \quad (1)$$

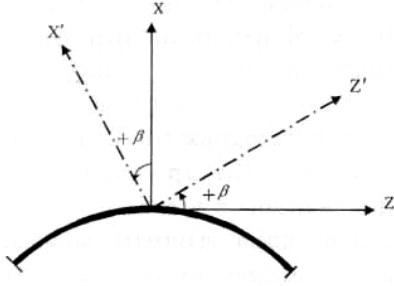


Fig. 4 Top view of dam and horizontal coordinates for input

ANALYTICAL METHOD

The computer program used in this study is EACD-3d-96 developed in UC at Berkeley by Chopra and Tan [10]. The program is based on substructure method and considers various effects such as: dam-foundation rock interaction, dam-water interaction, water compressibility and reservoir absorption.

Dam

The Morrow Point arch dam is selected for this study, because it has been investigated in detail by other researchers

analytically and experimentally [11] to obtain knowledge about dynamic characteristics of the dam. The dam, an almost perfectly symmetric single centered arch dam, is 144m high at its plane of symmetry and 244m wide at its crest. Its thickness at crest and base is 3.7m and 16m respectively. The results of two sets of forced vibration tests that had been conducted on the dam are summarized in the Table 1 [11].

The thick shell finite elements are used to model the main part of the dam body. In the part of the dam near its junction with the foundation rock, the dam is represented by transition elements (Fig. 5). The mass concrete in the dam is assumed to be homogeneous, isotropic and linear elastic with the following properties: Young's modulus $E_s = 27.579$ GPa, unit mass $\rho_s = 2483$ kg/m³, and Poisson's ratio $\nu_s = 0.2$. A constant hysteretic damping factor $\eta_s = 0.10$, which corresponds to 5 percent viscous damping in all natural vibration modes of the dam with empty reservoir on rigid foundation rock, is selected.

Foundation Rock

For the analysis of earthquake response of arch dam the frequency-dependent impedance (or dynamic stiffness) matrix, has been formulated for the foundation rock region, defined at the nodal point on the dam-foundation rock interface. A direct boundary element procedure has been used to determine the impedance matrix. For this direct boundary element procedure, the dam-foundation rock interface is discretized into a set of two-dimensional boundary elements with their nodal points matching the finite element idealization of the dam. The properties of the foundation rock are characterized by its Young's modulus E_f , Poisson's ratio ν_f ,

Table 1 Frequencies and dampings of vibration modes for Morrow Point Dam

Mode	Type	Forced vibration, June 1972		Forced vibration, June 1985	
		Frequency (Hz)	Damping values in percent of critical	Frequency (Hz)	Damping values in percent of critical
1	S	3.21	1.6	2.95	4
2	A	3.93	3	3.3	1.5
3	S			3.95	3.9
4	S			5.4	4.3
5	A	6.05	3	6.21	3.3
6	S	6.73	3.8	6.7	3.4
7	A	7.02	1.8		

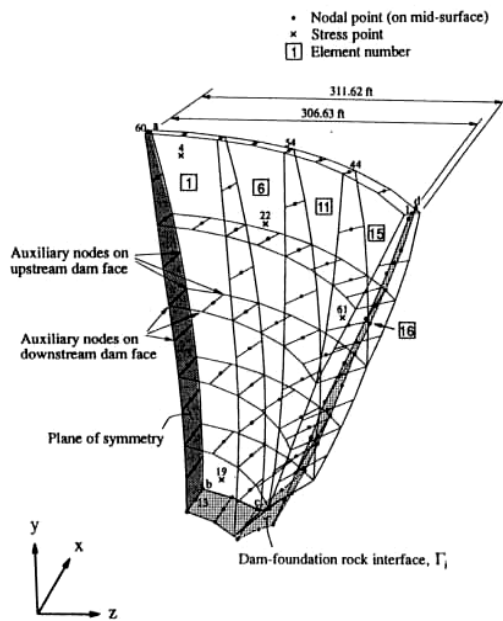


Fig. 5 Finite element mesh of one-half of Morrow Point Dam [10]

and unit mass ρ_f . The vibrational energy dissipation properties of the foundation rock are characterized by the constant hysteretic damping factor η_f . In this study the foundation rock is assumed to be homogeneous, isotropic, and viscoelastic with the following properties: unit mass $\rho_f = 2643 \text{ kg/m}^3$, Young's modulus $E_f = 27.579 \text{ GPa}$, Poisson's ratio $\nu_f = 0.2$,

and constant hysteretic damping factor $\eta_f = 0.10$, which corresponds to a viscous damping ratio of 5 percent.

Fluid Domain

The reservoir behind a dam is of complicated shape, as dictated by natural topography of the site, and extends several miles in the upstream direction. To efficiently recognize the long extent of the reservoir in the upstream direction, the fluid domain is idealized as a finite region of irregular geometry adjacent to the dam connected to an infinitely-long channel with uniform cross-section. The finite region of irregular geometry is idealized as an assemblage of three-dimensional finite elements, with the finite element mesh compatible with of the dam at its upstream face. For the infinite channel, a discretization of the cross-section, compatible with the discretization of the irregular region over the common cross-section combined with a continuum representation in the infinite direction provides for the proper transmission of pressure waves. The following properties are assumed for the impounded water: velocity of pressure waves $C = 1438.66 \text{ m/s}$ and unit mass $\rho = 1000 \text{ kg/m}^3$.

The boundary of a reservoir upstream from a dam typically consists of alluvium,

silt, and other sedimentary material. The absorption of hydrodynamic waves at the reservoir boundary can be represented approximately by a one-dimensional model, normal to the boundary and independent of the location on the boundary [13]. The fundamental parameter characterizing the effects of absorption of hydrodynamic pressure waves at the reservoir boundary is the admittance or damping coefficient $q = \rho / \rho_r C_r$ in which $C_r = \sqrt{E_r / \rho_r}$ where E_r is Young's modulus and ρ_r is the unit mass of the materials at the reservoir boundary. The wave reflection coefficient α , which is the ratio of the amplitude of the reflected hydrodynamic pressure wave to the amplitude of a normally propagating pressure wave incident on the reservoir boundary, is related to the damping coefficient q by [12]

$$\alpha = \frac{1 - q C}{1 + q C} \quad (2)$$

The wave reflection coefficient α is a more physically meaningful description than q regarding the absorption of hydrodynamic pressure waves at the reservoir boundary. Although the wave reflection coefficient depends on the angle of incidence of the pressure wave at the reservoir boundary, the value of α for normally incident waves as given by Eq. (2) is used for convenience. It is believed that α values from 1 to 0 would cover the wide range of materials encountered at the boundary of actual reservoirs. The reflection coefficient α is selected 0.5 in this study.

Number of Vibration Modes

The number of vibration modes required to represent the earthquake response of a dam is much less than the number of degree of freedoms in the finite

element system. Generally speaking, all the vibration modes that significantly contribute to the earthquake response of a dam should be included in the analysis. A few additional modes should also be included for accurate response result at high-frequency end of the frequency range.

The number of vibration modes required depends on the particular dam-water-foundation rock system and earthquake ground motion. In many cases, 15 vibration modes may be sufficient if the foundation rock is assumed rigid, and 15 to 20 modes may be sufficient if the foundation rock flexibility is included. Larger number of modes may be required, when foundation flexibility is high. In this study the number of required modes for convergence of solution have been checked by examining the change in the maximum stresses in the dam with an increase in the number of vibration modes included. If the stresses remain essentially unchanged then the number of vibration modes used in the previous analysis and the corresponding response results are satisfactory. In the current investigation up to 60 vibration modes of the dam have been considered, and variation of the maximum stresses have been examined with respect to number of vibration modes. Figure 6 shows the variation of maximum stresses with the number of vibration modes. For this case 30 vibration modes of the dam-foundation rock system were found to be sufficient to obtain accurate results. By considering 30 modes of vibrations we have checked our model by comparing computed frequencies of dam-water-foundation system with forced vibration measurement results. Table 2 shows the calculated results. Fairly good agreement was obtained for symmetric and anti-symmetric responses.

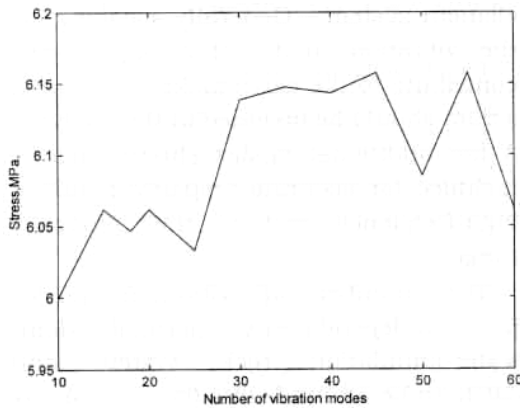


Fig. 6 Variation of stress in element 1 due to the number of modes of vibration

Table 2 Calculated frequencies and half-power damping values of vibration modes for Morrow Point Dam

Mode	Type	Frequency (Hz)	Damping values in percent of critical
1	S	2.87	1.2
2	A	3.21	3.4
3	S	3.84	9.4
4	S	5.34	4.1
5	A	6.29	
6	S	6.91	
7	A	7.17	1

EFFECTS OF DIRECTIVITY ON STRESSES

The arch and cantilever stresses of the all elements on the upstream and downstream face of the dam have been calculated for different incident angles (β) and compared in Tables 3 and 4, where maximums of the stresses under both static and dynamic loading conditions are shown. The stresses in the tables indicate the maximums of the stresses which vary with the rotation of the incident angle (β) of the input motion. The variation in the stresses are

exemplified in Fig. 7, in which maximum arch and cantilever stresses of the element 1 and 5 are plotted against the angle of incident.

Regarding the arch stress on the upstream face, the elements 1, 2 and 3 near the arch crown are most critical in intensity and the elements 15 and 16 near the abutment are the next. The stress increase from the minimum to the maximum is as large as 3 or 4 times near the arch crown, while it remains 2 times at most near the abutment. In the meantime, the cantilever stress on the upstream face is less than a half of the arch stress, and its maximum is seen in the element 5 located near the bottom of the dam. The increase in the cantilever stress is 3 times at most on the upstream face. It should be noted that the angle of incident where the stress becomes maximum is different between the arch and cantilever stresses, as can be seen in Fig. 7.

Regarding the stresses on the downstream face, both intensity and variation in the arch stress are largest in elements 11 and 12. Although the locations of the critical elements are different, the arch-stresses are almost the same in intensity as well as in variation as those on the upstream face. However, as for the cantilever stress, the maximum stress is seen in the element 5, as it is the case for upstream face, and the stress increase in the element 5 is almost twice. The maximum increase in the stress is seen in the element 10, which is more than 3 times.

After all, it has become evident that the directivity of the input motion has prominent but different effects on stresses of the dam body, dependent upon the location, in both intensity and variation, and the most critical angle of incident may be different, also dependent

Table 3 Arch and cantilever stresses on the upstream face of the dam with its maximum increase (in MPa)

Element No.	Arch St.	b	Arch St.	b	Increase	Cant. St.	b	Cant. St.	b	Increase
1	7.79	140	2.18	50	2.57	0.46	150	0.17	50	1.73
	8.06	140	2.1	50	2.85	0.62	-80	0.32	10	0.94
	9.15	130	2.2	50	3.16	0.74	-50	0.42	60	0.77
	8.34	130	2.24	50	2.72	0.46	140	0.23	50	1.01
2	7.42	140	1.71	50	3.33	0.83	-30	0.42	50	0.96
	6.44	140	1.28	50	4.02	1.04	-30	0.42	50	1.48
	7.56	130	1.47	50	4.14	1.34	-40	0.59	60	1.29
	8.63	130	1.81	50	3.78	1.01	-30	0.5	60	1.03
3	5.62	140	1.03	50	4.46	1.1	-40	0.4	50	1.77
	4.49	140	0.9	50	3.97	1.12	-40	0.39	50	1.88
	5.48	130	1.17	50	3.67	1.26	-40	0.43	50	1.96
	6.68	130	1.34	50	3.99	1.3	-40	0.51	40	1.53
4	3.62	140	0.82	50	3.4	1.01	-40	0.35	50	1.88
	2.33	130	0.6	50	2.91	1.12	-50	0.28	50	3.04
	3.4	140	0.8	50	3.23	1.06	-40	0.38	50	1.8
	4.65	130	1.06	50	3.38	1.07	-40	0.4	50	1.64
5	1.22	130	0.35	50	2.53	1.5	-40	0.45	50	2.31
	0.25	-30	0.12	50	1.07	2.23	120	0.79	50	1.8
	0.18	-50	0.06	50	2.07	2.84	-50	1.09	30	1.59
	2.09	130	0.5	50	3.22	1.45	-60	0.39	50	2.72
6	4.11	150	1.43	-90	1.88	0.29	120	0.11	50	1.65
	3.48	150	1.35	-90	1.57	0.62	80	0.25	-40	1.42
	5.16	150	1.82	-90	1.84	0.52	140	0.32	50	0.62
	5.15	150	1.73	70	1.99	0.28	-60	0.13	40	1.09
7	2.8	150	1.29	-90	1.17	0.83	20	0.35	120	1.36
	2.05	150	1.08	60	0.9	1.18	-10	0.41	-90	1.84
	4.08	150	1.37	50	1.98	1.26	-20	0.39	60	2.22
	4.79	150	1.73	50	1.77	0.89	-20	0.33	70	1.71
8	1.44	150	0.61	50	1.34	1.25	-10	0.38	-90	2.26
	0.68	150	0.34	10	1.02	1.32	-20	0.49	-90	1.69
	2.5	140	0.65	50	2.86	1.35	-30	0.35	50	2.85
	3.45	150	1.05	50	2.28	1.3	-20	0.33	50	2.88
9	0.42	40	0.28	150	0.5	1.43	-30	0.46	50	2.13
	0.71	150	0.26	80	1.75	1.14	-20	0.41	50	1.78
	0.62	140	0.29	20	1.15	1.23	-30	0.37	50	2.36
	1.69	140	0.48	50	2.48	1.3	-30	0.38	50	2.42
10	0.63	150	0.26	70	1.39	1.72	-40	0.53	50	2.22
	0.94	150	0.31	-90	2.06	1.68	-40	0.56	50	1.97
	0.77	130	0.3	50	1.56	1.95	130	0.62	50	2.17
	0.32	-60	0.18	50	0.76	1.58	-40	0.5	50	2.19
11	2.05	-40	1.03	60	1	0.25	80	0.08	-20	2.01
	1.37	-50	0.74	50	0.86	0.85	80	0.35	10	1.44
	1.96	-30	1.21	-90	0.63	0.82	70	0.27	-40	1.98
	2.45	-30	1.26	-90	0.94	0.31	80	0.12	-10	1.57
12	1.03	-90	0.48	-10	1.14	1.31	50	0.69	-10	0.89
	1.77	80	0.49	-20	2.61	1.29	40	0.76	-10	0.69
	0.77	-80	0.51	50	0.53	1.15	30	0.52	-80	1.22
	1.4	-40	0.87	60	0.61	1.01	40	0.39	-70	1.57
13	1.78	70	0.63	-30	1.85	1.18	20	0.63	-40	0.86
	1.22	50	0.41	-50	1.95	1.21	0	0.48	-90	1.49
	1.07	150	0.45	-80	1.37	1.46	-20	0.44	-90	2.36
	0.63	60	0.39	150	0.64	1.34	-10	0.39	-90	2.46
14	0.91	150	0.29	-60	2.14	1.09	-20	0.37	-90	1.92
	0.97	50	0.34	-50	1.88	1.05	-20	0.36	-90	1.95
	0.91	150	0.28	-70	2.26	1.07	-20	0.41	-90	1.59
	1.1	150	0.3	-80	2.63	1.26	-20	0.43	-90	1.97
15	5.12	120	1.62	50	2.15	1.28	110	0.56	40	1.28
	5.16	110	2.25	40	1.29	1.74	-90	0.93	20	0.86
	2.71	-80	1.01	20	1.67	1.24	-90	0.61	20	1.03
	3.5	120	1.16	50	2	0.62	-90	0.29	20	1.15
16	3.48	-80	1.45	20	1.4	1.52	-90	0.84	10	0.82
	4.5	100	1.88	30	1.39	1.73	-90	0.89	20	0.95
	3.31	-90	1.31	20	1.54	1.39	60	0.82	0	0.7
	2.75	-90	1.02	20	1.7	1.53	-90	0.88	10	0.74

Table 4 Arch and cantilever stresses on the downstream face of the dam with its maximum increase (in MPa)

Element No.	Arch St.	b	Arch St.	b	Increase	Cant. St.	b	Cant. St.	b	Increase
1	1.72	-80	1.04	-10	0.65	0.34	-60	0.19	20	0.83
	1.78	60	0.78	130	1.29	0.54	110	0.28	-50	0.95
	2.28	-10	1.01	90	1.25	0.54	130	0.31	70	0.76
	1.5	30	0.98	120	0.53	0.38	-60	0.21	20	0.81
2	1.86	70	0.68	-30	1.72	0.55	-40	0.3	60	0.85
	1.81	80	0.56	-30	2.24	0.76	-50	0.29	70	1.57
	1.57	0	0.74	100	1.14	0.67	150	0.38	80	0.75
	2.06	0	0.87	80	1.36	0.57	150	0.34	80	0.67
3	1.77	90	0.5	-20	2.52	0.6	140	0.24	50	1.46
	1.62	100	0.42	-10	2.82	0.55	140	0.21	50	1.66
	0.7	0	0.37	120	0.89	0.6	140	0.24	50	1.47
	1.15	0	0.59	110	0.96	0.64	140	0.32	-20	1.03
4	1.46	110	0.39	-10	2.77	0.4	140	0.18	-50	1.16
	1.17	110	0.35	0	2.31	0.33	130	0.18	-90	0.81
	0.52	-50	0.28	50	0.83	0.6	-40	0.32	50	0.87
	0.56	-60	0.3	120	0.89	0.47	-20	0.27	-90	0.74
5	0.84	120	0.28	0	1.97	0.46	140	0.12	50	2.95
	0.45	130	0.17	10	1.71	1.7	140	0.39	50	3.31
	0.19	-60	0.06	50	1.89	1.99	140	0.49	50	3.06
	0.47	-50	0.22	50	1.18	0.42	130	0.19	50	1.17
6	5.87	110	2.25	40	1.61	0.27	-80	0.13	-40	1.06
	6.61	110	2.63	30	1.52	0.52	70	0.24	-50	1.22
	4.91	100	1.51	20	2.25	0.46	-50	0.32	40	0.41
	4.81	-70	1.56	30	2.08	0.31	120	0.18	60	0.74
7	6.63	110	2.44	40	1.72	0.76	150	0.26	-90	1.97
	6.28	120	2.2	40	1.85	1.02	150	0.32	80	2.16
	4.23	110	1.32	20	2.19	0.89	-40	0.29	80	2.02
	4.59	100	1.39	20	2.3	0.76	-40	0.3	60	1.52
8	5.95	120	1.88	50	2.16	1.02	150	0.32	70	2.19
	5.34	130	1.54	50	2.47	1.1	150	0.32	50	2.38
	3.5	120	1.07	20	2.27	0.74	140	0.15	50	4.09
	3.93	110	1.21	20	2.24	0.85	150	0.24	50	2.6
9	4.74	130	1.34	50	2.53	0.89	140	0.19	50	3.62
	3.75	130	1.01	50	2.72	1.25	140	0.25	50	4.04
	2.57	130	0.79	20	2.27	0.57	140	0.1	50	4.67
	3.1	120	0.93	20	2.35	0.59	130	0.09	50	5.6
10	2.4	130	0.67	50	2.56	1.39	140	0.3	50	3.72
	2.87	130	0.75	50	2.82	1.41	140	0.31	50	3.59
	1.84	130	0.5	50	2.68	1.59	140	0.36	50	3.44
	2.3	130	0.71	30	2.22	1.09	140	0.21	50	4.27
11	7.59	130	0.78	50	3.26	0.17	50	0.09	-90	0.84
	7.8	130	1.81	50	3.31	0.74	-90	0.39	0	0.91
	8.17	120	2.38	50	2.44	0.59	60	0.23	-30	1.57
	7.53	130	1.98	50	2.81	0.25	60	0.12	-90	1.07
12	7.3	130	1.62	50	3.5	1.07	50	0.52	110	1.06
	6.83	140	1.46	50	3.68	1.33	50	0.71	-60	0.88
	7.45	130	1.89	50	2.95	0.93	150	0.31	-70	1.99
	7.82	120	2.08	50	2.77	0.76	40	0.26	-50	1.9
13	6.46	140	1.61	50	3.02	1.16	10	0.38	-90	2.01
	6.33	140	1.3	50	3.87	1.47	150	0.58	60	1.54
	5.39	130	1.37	50	2.94	1	150	0.32	-90	2.1
	6.9	130	1.7	50	3.07	1.09	150	0.34	-90	2.24
14	5.23	140	1.16	50	3.51	1.44	140	0.43	50	2.37
	6.14	140	1.25	50	3.91	1.64	140	0.54	50	2.06
	4.84	140	1.06	50	3.55	1.54	140	0.37	50	3.17
	4.69	130	1.16	50	3.02	1.11	140	0.36	50	2.07
15	3.62	0	1.67	-90	1.16	1.03	-80	0.45	30	1.31
	3.9	10	1.53	-90	1.55	1.29	-90	0.76	10	0.7
	5.79	150	1.82	50	2.18	0.99	50	0.53	130	0.86
	5.58	150	1.62	50	2.44	0.52	50	0.28	0	0.85
16	5.35	150	2.22	-90	1.41	1.5	50	0.89	120	0.69
	4.46	10	1.6	-90	1.79	1.5	50	0.94	150	0.61
	5.69	150	2.38	-90	1.39	1.55	50	0.88	-40	0.75
	6.21	150	2.14	50	1.91	1.37	50	0.8	120	0.72

upon the location as well as the kind of stresses such as arch and cantilever stresses. Thus, for an arch dam located in near-field, the effects of the directivity needs to be taken into account in seismic design, and further studies to its implementation is needed.

EFFECTS OF VERTICAL GROUND MOTION

In the case of far-field ground motions, if the reservoir is empty, the contribution

of the response to the vertical component is very small whether the foundation rock is rigid or flexible. For the dam with impounded water and, the response to the vertical component of ground motion and its contribution to total response depends on coefficient of absorption. We have considered the response of Morrow Point Dam to vertical ground motion recorded at Pacoima Dam Station with $\alpha = 0.5$, and the results are shown in Fig. 8. For this special case because the vertical and horizontal components are not in phase, and the vertical to horizontal

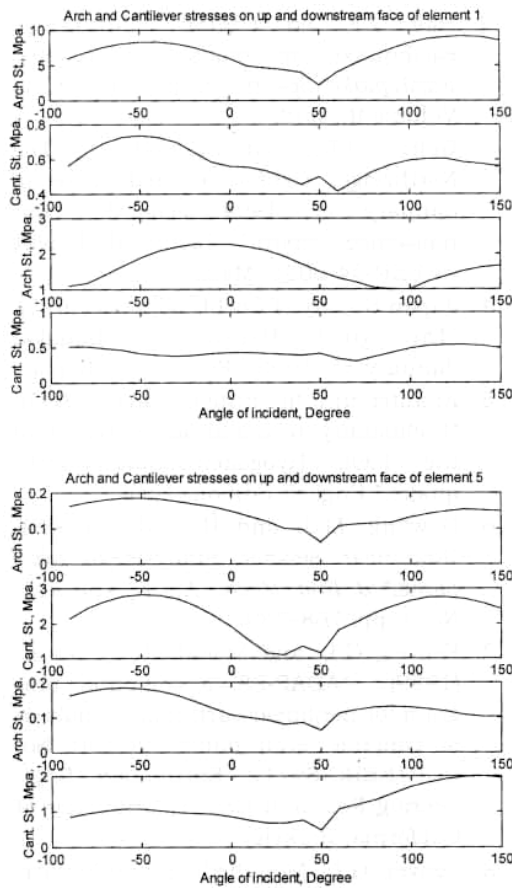


Fig. 7 Variation of arch and cantilever stresses with the angle of incident

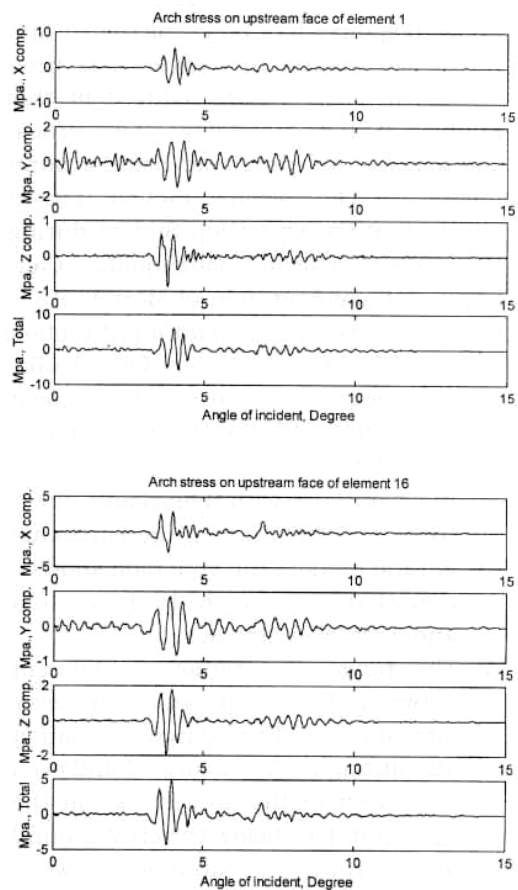


Fig. 8 Contribution of vertical component of ground motions to total response

acceleration ratio is small, the contribution of vertical ground motion to total response is about 30%. But for other near-field ground motions with large V/H ratio, large contribution has been observed from vertical ground motion even for smaller coefficient of absorption, α . This will be the subject of the future detailed study on the effect of vertical ground motion.

CONCLUDING REMARKS

To evaluate near-field effects of input ground motion on stresses of arch dam, linear response has been calculated and range of variation in stresses has been examined. The effects focused in this study are the directivity and vertical component of the near-field ground motion. The strong motion record observed at Pacoima Dam Station during the 1994 Northridge earthquake, California and configuration of Morrow Point Dam have been used as an input motion and a model of an arch dam for the sake of convenience. As far as the present study is concerned, the following conclusions can be drawn.

1. In accordance with remarkable directivity or polarization in the horizontal ground motion, the arch dam shows a remarkable variation in both arch and cantilever stresses.
2. The range of variation is different between the arch and cantilever stresses. The large variation amounting to the factor of 3 and even 4, is seen in the arch stress on the upstream face below the crest around arch crown or abutment, while similar amount of variation in the cantilever stress is seen on the downstream face near the deepest bottom.
3. The most critical angle of incident at which the largest stress is attained in the response is not always the same through the dam body.
4. The contribution of the vertical component to the total response is about 30%.

REFERENCES

1. Earthquake Engineering Research Institute, EERI (1994). "Northridge Earthquake — January 17, 1994 Preliminary Reconnaissance Report," Oakland, California.
2. Hall, J.F., ed. (1995). "Northridge earthquake reconnaissance report," *Earthquake Spectra*, Supplement C to Volume II, April.
3. Goltz, J.D., ed. (1994). "The Northridge, California earthquake of January 17, 1994: general reconnaissance report," Technical Report NCEER-94-0005, March.
4. Japan Society of Civil Engineers (1995). "The great Hanshin earthquake, January 17, 1995," Preliminary Report.
5. Architectural Institute of Japan (1995). "Preliminary reconnaissance report of the 1995 Hyogoken-Nanbu earthquake," English Edition, April.
6. Dowling, M.J. and Hall, J.F. (1989). "Nonlinear seismic analysis of arch dams," *J. Eng. Mech.*, ASCE, Vol. 115, No. 4, pp. 768–789.
7. Fenves, G.L. and Mojtahedi, S., et al. (1989). "ADAP-88: a computer program for nonlinear earthquake analysis of concrete arch dams," Report No. UCB/EERC-89/12, Earthquake Engineering Research Center, University of California, Berkeley.
8. Fenves, G.L., Mojtahedi, S. and Reimer, R.B. (1992). "Effect of contraction joints on earthquake response of arch dams," *J. Structural Engineering*, ASCE, Vol. 118, No. 4, pp. 1039–1055.

9. Nowak, P.S., and Hall, J.F. (1990). "Arch dam response to nonuniform seismic input," *J. Eng. Mech.*, ASCE, Vol. 116, No. 1, pp. 125–139.
10. Tan, Hanchen and Chopra, A.K. (1996). "EACD-3D-96 — A computer program for three-dimensional earthquake analysis of concrete dams," Report No. UCB/SEMM-96/06, Dept. of Civil and Environmental Eng. University of California, Berkeley.
11. Hall, J.F. (1988). "The dynamic and earthquake behavior of concrete dams: review of experimental behavior and observational evidence," *Soil. Dyn. Earth. Eng.*, Vol. 7, No. 2, pp. 58–121.
12. Hall, J.F. and Chopra, A.K. (1983). "Dynamic analysis of arch dams including hydrodynamic effects," *J. Eng. Mech.*, ASCE, 109, pp. 149–167.
13. Fenves, G. and Chopra, A.K. (1984). "Earthquake analysis of concrete gravity dams including reservoir bottom absorption and dam-water-foundation rock interaction," *Earth. Eng. Struc. Dyn.*, 12, pp. 663–680.